

Structure of casein micelles studied by small-angle neutron scattering

Steen Hansen¹, Rogert Bauer¹, Stig Bredsted Lomholt², Karsten Bruun Quist², Jan Skov Pedersen³, Kell Mortensen³

¹ Department of Mathematics and Physics, Royal Veterinary and Agricultural University, Thorvaldsensvej 40, DK-1871 Frederiksberg C, Denmark

² Institute for Dairy Research, Royal Veterinary and Agricultural University, Howitzvej 11, DK-2000 Frederiksberg, Denmark

³ Department of Solid State Physics, Risø National Laboratory, DK-4000 Roskilde, Denmark

Received: 13 October 1994 / Accepted in revised form: 13 October 1995

Abstract. The structure of casein micelles has been studied by small-angle neutron scattering and static light scattering. Alterations in structure upon variation of pH and scattering contrast, as well as after addition of chymosin, were investigated. The experimental data were analyzed by a model in which the casein micelle consists of spherical submicelles. This model gave good agreement with the data and gave an average micellar radius of about 100–120 nm and a submicellar radius of about 7 nm both with a polydispersity of about 40–50%. The contrast variation indicated that the scattering length density of the submicelles was largest at the center of the submicelles. The submicelles were found to be closely packed, the volume fraction varying slightly with pH. Upon addition of chymosin the submicellar structure remained unchanged within the experimental accuracy.

Key words: Casein – Small-angle neutron scattering

1. Introduction

The caseins constitute approximately 80% of the protein normally found in bovine milk and are divided into α_{s1} -, α_{s2} -, β - and κ -casein. In milk the caseins are found in large aggregates of casein molecules, called casein micelles, which also contain mineral constituents, especially calcium phosphate. The radius of casein micelles is typically 50–200 nm. κ -casein is located predominantly at the surface of the micelles and has a hydrophilic tail which protrudes into solution and provides steric stabilization of the micelle (see e.g. Israëlachvili 1991). The structure of these casein micelles has been the subject of many studies (e.g. Schmidt et al. 1974; Stothard and Cebula 1982; Visser et al. 1986; Stothard 1989; de Kruif and May 1991). From these studies several models for casein micelles have been suggested. One model for the micelle (reviewed by McMahon and Brown 1984 and Schmidt 1982) is a sphere comprised of spherical submicelles with an average diameter of 8–20 nm. Other models suggest the micelles consist of a continuous network with

subdomains of higher density corresponding to the submicelles of the previous model (e.g. Visser et al. 1986).

During cheese production chymosin, a proteolytic enzyme that splits the Phe₁₀₅-Met₁₀₆ bond of κ -casein, is added to the milk. The hydrophilic part of κ -casein, called the Caseino Macro Peptide (CMP), is released into solution after proteolysis. CMP contains most of the peptide that protrudes from the surface of the micelle. This proteolysis leads to loss of steric stabilization as well as electrostatic repulsion and results in aggregation and subsequent gelation of the casein. The structure of the gel formed during the coagulation process is of great importance to the structure and rheological properties of the final cheese. From electron microscopic investigations it is known that after a gel has been formed the micelles gradually fuse and after some hours the individual micelles can no longer be distinguished (Roefs et al. 1990). It is not known, however, to what degree the internal structural elements remain intact after coagulation.

In yoghurt and other acidified dairy products, the coagulation of casein is achieved by decreasing the pH. The structure of the acid gel is in many ways comparable to the structure of a chymosin gel, but the rheological characteristics are different. Acidification leads to the release of calcium phosphate from the micelles and might be expected to change the internal structure of the micelles.

The effect of addition of chymosin and acidification on the internal structure of casein micelles is thus an important parameter affecting the properties of many dairy products and the aim of this work was to study these changes by means of small-angle neutron scattering.

Using small-angle neutron scattering (SANS) for measurements on casein micelles we were able to cover five orders of magnitude in intensity by fitting the data corresponding to different settings of the SANS instrument simultaneously. This allowed us for the first time to obtain information about the micellar as well as the submicellar structure simultaneously as we cover a size range of about 2 to 200 nm. By including data from static light scattering we are able to increase the size range studied up to about 1000 nm. Using contrast variation allowed us to extract further information from the SANS experiment and by measuring at high and low pH the effects of acidification were investi-

Model of Casein Micelle

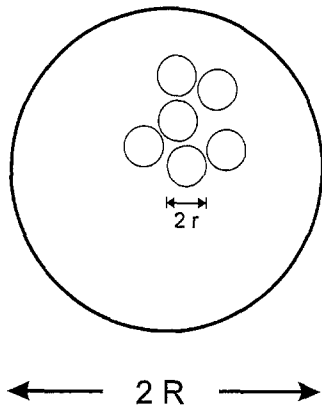


Fig. 1. Model of casein micelle

gated. For analysis of the data we found the model containing spherical submicelles to be consistent with our measured data. To improve the model fit we included polydispersity in the model both for the spherical micelles and for the spherical submicelles. With this modification we obtained good agreement with the experimental data. Using contrast variation we were able to demonstrate inhomogeneities in the scattering length density of the submicelles. The aggregation behaviour after the addition of chymosin was also studied by static light scattering and this confirmed the somewhat surprising indication from the SANS data, that no change in the size range accessible by SANS appeared upon aggregation of the micelles thus confirming the structural stability of the submicelles.

2. Theory

2.1. Small-angle scattering

The casein model used for the analysis of the SANS data is shown in Fig. 1. The casein micelles are assumed to be polydisperse with a Gaussian size distribution having average radius R and width σ_R . Likewise the submicelles are assumed to be polydisperse with average radius r and width σ_r . Assuming a micelle to consist of n submicelles leads to an average volume fraction of $\eta = n \cdot r^3 / R^3$. The fitted parameters are therefore $(R, \sigma_R, r, \sigma_r, \eta)$. Owing to small experimental errors in the determination of background and absolute calibration, a constant background and a factor for each measured spectrum were included in the set of fitting parameters. This gave only minor corrections to the measured spectra.

For the length of the scattering vector $q = 4\pi \sin \theta / \lambda$, where θ is half the scattering angle and λ is the wavelength of the neutrons, the measured intensity $I(q)$ is modelled by the Debye formula

$$I(q) \propto \sum_{i=1}^n \sum_{j=1}^n f_i(q) f_j(q) \frac{\sin(qr_{ij})}{qr_{ij}} \quad (1)$$

where f_j is the form factor for the scatterer j , r_{ij} is the distance between scatterers i and j and n is the total number

of scatterers. Assuming the micelle to consist of spherical micelles of radius r and uniform scattering density Eq. (1) can be written as

$$I(q) \propto P_{\text{sphere}}(q, r) \left(n + \sum_{i=1}^n \sum_{j=1}^{n'} \frac{\sin(qr_{ij})}{qr_{ij}} \right) \quad (2)$$

by writing $f_i^2(q) = P_{\text{sphere}}(q, r)$ and where the prime indicates that contributions having $j = i$ are to be excluded. For $n \rightarrow \infty$ the double sum in Eq (2) will tend towards $n^2 P_{\text{sphere}}(q, R)$. However as the submicelles have a finite size n will be limited and r_{ij} only takes values larger than the diameter of the smallest submicelle. The effects from this will only be minor in the scattering profile as the large polydispersity of the submicelles will have a strong smearing effect upon peaks in the structure factor for the submicelles (see Pedersen, 1994). Therefore Eq. (2) can be approximated by

$$I(q) \propto P_{\text{sphere}}(q, r) (n + n^2 P_{\text{sphere}}(q, R)). \quad (3)$$

Including polydispersity the measured intensity is then given as

$$I(q) \propto I_{\text{sphere}}(q, r, \sigma_r) (1 + n I_{\text{sphere}}(q, R, \sigma_R)) \quad (4)$$

where $I_{\text{sphere}}(q, x, \sigma_x)$ is the scattered intensity from a Gaussian size distribution of spheres with mean radius x and width σ_x . This is valid as the radius of the submicelle is much smaller than the radius of the micelle (typically $r < 0.1R$) and consequently the effects from the polydispersity pertain to different q -ranges.

The molecular mass can be calculated from

$$M = \frac{I(0)}{C N_A \overline{\Delta\rho}^2} \quad (5)$$

where C is the protein concentration, N_A is Avogadro's number and $\overline{\Delta\rho}$ is the average scattering length density per unit mass.

From the integral invariant $Q = \int q^2 I(q) dq$ the volume of the scatterer can be calculated according to $V = 2(\pi^2 I(0)/Q) \overline{\Delta\rho}^2 / \overline{\Delta\rho}^2$ which by comparison with the volume calculated from the model of the micelle allows the internal density fluctuations to be calculated.

3. Experimental

3.1. Small-angle neutron scattering

The SANS measurements were carried out at the facility at the DR3 reactor at the Risø National Laboratory in Denmark. In the present experiments the scattering patterns were recorded in the q -range 0.017–1.8 nm⁻¹, using four instrument settings. The raw spectra were corrected for background from buffer, cuvette, and other sources by conventional procedures. The intensities were converted to an absolute scale and corrected for variations in detector efficiency by dividing by the scattering spectrum of pure water. The data were normalized by the protein concentration. Throughout the data analysis the instrumental smearing of the ideal cross section was included as described in Pedersen et al. (1990).

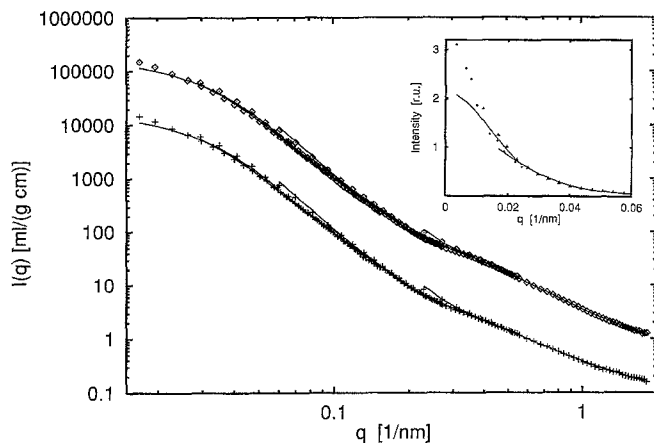


Fig. 2. Casein data pH 6.7 (diamonds) and fit (full line), casein data pH 5.7 (+) and fit (full line) shifted vertically one decade for clarity. Insert shows static light scattering data (+), SANS data (triangles) and fit (full line) on linear scale. All data in 100% D₂O

3.2. Static light scattering

Static light scattering measurements were carried out in a DAWN F light scattering photometer (Wyatt Technology, Santa Barbara, USA). A 67 μl flow cell designed especially to give access to very low angles was used. Scattered light was monitored at 15 angles from 4.25° to 143.76°. The light source was a 5 mW 632.8 nm He-Ne laser (the intensity was reduced by neutral filters when appropriate to give suitable detector readings). Initially the scattered intensities from all angles were normalized to give the same value using the scattered intensities from a sample of human insulin purified by gel permeation chromatography prior to the measurement and dissolved in 0.1 M NaCl at pH 7.0, assuming insulin to be an isotropic scatterer under these conditions.

3.3. Preparation of samples

Skim milk was prepared by dissolving 9 g of low heat skim milk powder in 100 g of 100, 72, 42 or 0% D₂O respectively (0% D₂O = 100% H₂O) and thoroughly mixing for 10 min. The pH values given in this work are the readings of a conventional pH-meter. The pH was 6.6 in H₂O, but 6.7 in D₂O. For the low pH sample the pH was adjusted by addition of 1 M HCl in D₂O to 5.7. The reconstituted milk was kept at 4°C until used for SANS. The casein content of the reconstituted milk was 25 mg/ml. Milk permeate for background measurements was prepared by ultrafiltration of the skim milk through a Milipore PTHK membrane in a 76 mm diameter Amicon model 8400 stirred pressurized cell (Amicon, USA). In the aggregation experiment 0.02% of a standard chymosin solution was added to the milk. The chymosin used was Chymogen, 66 CHU/ml (Chr. Hansen Lab., Hørsholm, DK). The samples for light scattering were prepared as described for SANS, but diluted 1000 times in permeate.

4. Results

Figure 2 shows the result of a SANS experiment consisting of four different spectra at two pH values and the corre-

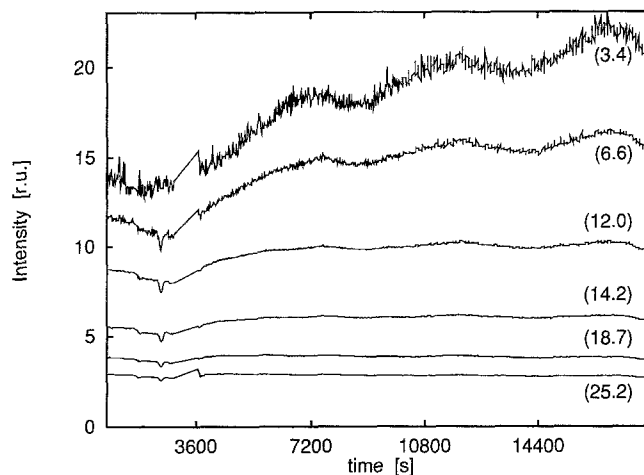


Fig. 3. Static light scattering intensity at 6 different angles as a function of time for chymosin-induced aggregation of casein micelles at pH 6.7, 100% D₂O and 1000 times dilution. The q -values (in μm^{-1}) corresponding to the different angles are shown in the figure

sponding fit to the data. The four spectra corresponding to the four different settings were fitted simultaneously using different resolution functions for the different settings which gives rise to the discontinuities in the fits.

The data in the upper curve were measured at pH 6.7 and the radius of the casein micelle calculated from the model is 100 nm with a polydispersity of 50%. The radius of the submicelle was found to be 7 nm, also with a polydispersity of 50%. The volume fraction was found to be 0.8.

Including static light scattering (shown as insert in Fig. 2) our simple model was immediately able to fit all the highest q -values without any significant change in the fitting parameters. Only the three lowest scattering vectors indicated larger sizes for the casein micelles and this could be explained by deviations from the Gaussian size distribution assumed (a tail in the size distribution for the micelles giving larger micelles than predicted by the Gaussian distribution would have this effect upon the measured intensity) - or by a small degree of aggregation.

From the contrast variation (see below) we found the average value for the contrast of the micelle to be $\overline{\Delta\rho} = 3.6 \cdot 10^{-14}$ cm/D and from Eq (5) the apparent molecular weight was found to $M \approx 1.4 \cdot 10^8$ D.

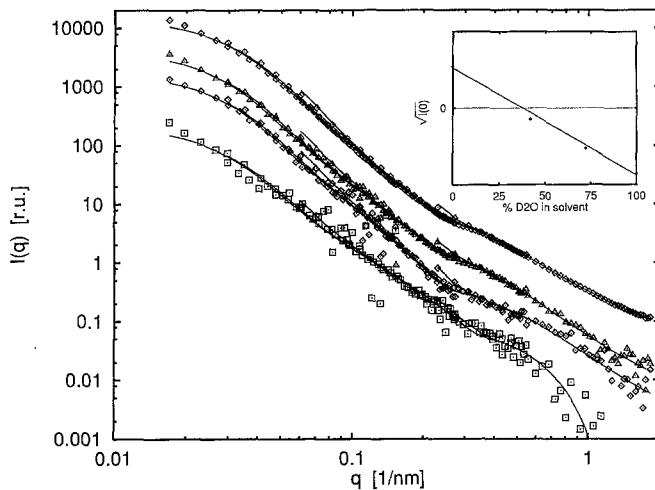
Light scattering experiments done with casein micelles in 100% H₂O and 100% D₂O showed that there was no difference in the structure of the micelles between these solvents.

4.1. Change in pH

For a pH value of 5.70 the data shown in the lower curve of Fig. 2 were measured. The radius of the micelle and the molecular weight remained unchanged within the experimental accuracy, but the radius of the submicelle increased slightly to about 8 nm. Also the volume fraction increased to 1.1.

Table 1. Effect of contrast variation on the parameters of the model for casein micelle

D ₂ O [%]	R [nm]	σ_R [nm]	r [nm]	σ_r [nm]	η
0	115	49	4.5	2.2	0.53
42	119	53	4.1	–	0.21
72	125	54	6.3	3.0	0.54
100	101	42	6.7	3.7	0.80

**Fig. 4.** Contrast variation. Markers show scattering intensities and full lines show fits for (from top) 100, 72, 0 and 42% D₂O respectively. Insert shows $\sqrt{I(0)}$ as a function of contrast

4.2. Addition of chymosin

Upon the addition of chymosin the casein micelles aggregated (by visual inspection it was checked after each experiment – about 20 hours – that a gel had formed), but no change in the structure of the submicelles was detected by SANS. Figure 3 shows static light scattering from casein micelles at 6 different angles. The corresponding q -values are given in the figure (in μm^{-1}). Rennet was added at $t = 2500$ s. The discontinuity in the curves at 3000-3600 seconds is due to an air bubble in the sample cell at this time. The short term fluctuations in the signal are due to counting statistics and the long term fluctuations are most likely due to variations in the aggregation rate. From the figure it is seen that at the highest scattering angles no change in the scattered intensity is observed. This is in good agreement with the results of the SANS measurements as $25.2 \mu\text{m}^{-1} \approx 0.025 \text{ nm}^{-1}$ which is of the order of the smallest q -values accessible by our SANS measurements.

4.3. Contrast variation

Figure 4 shows measurements and corresponding fits at 4 different contrasts: 0, 42, 72 and 100% D₂O respectively. The parameters obtained from the fits are given in Table 1. From the absolute intensities the matching point can be deduced from a linear fit to $\sqrt{I(0)}$ as a function of the contrast, as shown in the insert to Fig. 4. The measured matching point corresponds to 38% D₂O $\approx 3.6 \cdot 10^{-14} \text{ cm/D}$.

5. Discussion

From our measurements on intact casein micelles over 5 orders of magnitude in intensity the dimensions of the casein micelles as well as of the submicelles agree well with previous measurements using a restricted q -range and/or measurements on submicelles only (Stothard and Cebula 1982; Stothard 1989; de Kruif and May 1991).

From the calculation of the integral invariant in 100% D₂O we find $\overline{\Delta\rho^2}/\overline{\Delta\rho}^2 = 1.7$. This clearly demonstrates that the micelles are not homogeneous scatterers, but have very large internal density variations which is also evident from the contrast variation experiments.

Our values for the radius of the submicelles in 100% D₂O – 7 nm for pH 6.7 changing to about 8 nm for pH 5.70 – are in good agreement with literature values (see e.g. Stothard 1989, and references therein).

Our matching point of about 38% D₂O for the casein micelle agrees well with that of Stothard and Cebula (1982) who for submicelles alone found a matching point of 40.7 ± 0.5 % D₂O. As the scattering contrast of the solvent approaches that of the matching point, the fitted radii of the submicelle decreases, indicating that it is mainly the surface of the submicelles which is matched at this contrast.

From the measured radius of gyration for the submicelles alone as a function of scattering contrast, Stothard and Cebula (1982) found the scattering length density for the submicelles to be largest at the center of the submicelles. This is also in accordance with our findings as – neglecting the measurement closest to the matching point – the smallest diameter of the submicelle is found for the lowest scattering length density of the solvent. Because of the low scattering intensity close to the matching point, the dimensions deduced for the submicelles in 42% D₂O are very uncertain.

The width of about 50% for the Gaussian size distribution for the submicelles shows a large degree of polydispersity. From measurements on submicelles Stothard and Cebula (1982) obtained a radius of gyration of $R_g = 6.5$ nm corresponding to a radius of the submicelles of approximately 8.4 nm. Stothard and Cebula (1982) found that measurements on whole casein micelles indicated a close packing of the submicelles due to the measured inflection in the scattering curve at $q \approx 0.35 \text{ nm}^{-1}$. This was supported by Stothard (1989) who fitted a close packing model for the submicelles to the scattered intensity of casein micelles using the experimental intensity form factor for the submicelles. These measurements were limited to about two decades in intensity and less than one decade for the length of the scattering vector. We note that in spite of the differences in experimental set up and in the models used we obtain almost identical results.

Our values of 0.8-1.1 for the volume fraction in 100% D₂O is in agreement with a close packing of the submicelles as reported in previous studies. The fact that the volume fraction obtained from the fitting procedure exceeds the theoretical maximum for closely packed spheres could be explained by interpenetration of the submicelles (they are not hard spheres) and the polydispersity of the spheres (allowing a much closer packing) as well as deficiencies of the very simple model. The increased volume fraction of the

submicelles at low pH-values is consistent with the swelling reported by, for example, Roefs et al. (1986).

6. Conclusion

By using SANS and static light scattering we have obtained structural information about casein micelles during various conditions. Our data measured over five orders of magnitude in intensity are in good agreement with previous measurements and they strongly support a specific model for the casein micelle as consisting of closely packed spherical submicelles of inhomogeneous scattering density. In addition to this we have demonstrated the stability of the submicellar structure upon addition of chymosin and/or change of pH.

Acknowledgements. We thank Dr. D. S. Horne, Hannah Research Institute, Ayr, UK for providing the skim milk powder. This work is part of the FØTEK programme supported by the Danish Government and the Danish Dairy Board.

References

1. Hooydonk van ACM, Hagedorn HG, Boerrigter IJ (1986) *Neth Milk Dairy J* 40:281–286
2. Israelachvili JN (1991) *Intermolecular and surface forces* (2nd edn) Academic Press, London
3. Kruif de CG, May RP (1991) κ -Casein micelles: structure, interaction and gelling studied by small-angle neutron scattering. *Eur J Biochem* 200:431–436
4. Martin JE, Hurd AJ (1987) Scattering from fractals. *J Appl Crystallogr* 20:61–78
5. McMahon DJ, Brown RJ (1984) Enzymatic coagulation of casein micelles: A review. *J Dairy Sci* 67:919–929
6. Pedersen JS (1994) Determination of Size Distributions from Small-Angle Scattering Data for Systems with Effective Hard-Sphere Interactions. *J Appl Crystallogr* 27:595–608
7. Pedersen JS, Posselt D, Mortensen K (1990) Analytical treatment of the resolution function in small-angle scattering. *J Appl Crystallogr* 23:321–333
8. Roefs SPFM, Walstra P, Dalgleish DG, Horne DS (1985) Preliminary note on the change in casein micelles caused by acidification. *Neth Milk Dairy J* 39:119–122
9. Roefs SPFM, van Vliet T, van den Bijgaart HJCM, de Groot-Mostert AEA, Walstra P (1990) Structure of casein gels made by combined acidification and rennet action. *Neth Milk Dairy* 44:159–188
10. Schmidt DG (1982) Association of caseins and casein micelle structure. In: *Development in dairy chemistry*. Fox PF, (ed.) Applied Science Publication, London, pp 61–86
11. Schmidt DG, Both P, van Markwijk BW, Buchheim W (1974). The determination of size and molecular weight of casein micelles by means of light scattering and electron microscopy. *Biochim Biophys Acta* 365:72–79
12. Stothart PH (1989) Subunit structure of casein micelles from small-angle neutron-scattering. *J Mol Biol* 208:635–638
13. Stothart PH, Cebula DJ (1982) Small-angle neutron scattering study of bovine casein micelles and sub-micelles. *J Mol Biol* 160:391–395
14. Visser J, Minihan A, Smits P, Tjan SB, Heertje I (1986) Effects of pH and temperature on the milk salt system. *Neth Milk Dairy J* 40:351–368